

## Conference Paper

# Polarization Reversal by Tip of Scanning Probe Microscope in SBN

E.A. Neradovskaya<sup>1</sup>, M.M. Neradovskiy<sup>1</sup>, V.V. Fedoroviyh<sup>1</sup>, A.P. Turygin<sup>1</sup>, V.Ya. Shur<sup>1</sup>, A.L. Kholkin<sup>1,2</sup>, and I.L. Ivleva<sup>3</sup>

<sup>1</sup>Institute of Natural Sciences, Ural Federal University, 620000 Ekaterinburg, Russia

<sup>2</sup>Department of Physics & CICECO – Materials Institute of Aveiro, University of Aveiro, 3810-193 Aveiro, Portugal

<sup>3</sup>Prokhorov General Physics Institute of the RAS, 119991 Moscow, Russia

## Abstract

We present the results of experimental study of the influence of initial domain state on the shape and size of isolated domains created by the conductive tip of scanning probe microscope during local polarization reversal in relaxor ferroelectric strontium barium niobate doped with nickel and cerium. The domain radius was found to increase with increasing voltage and time and depend on the initial polarization direction. Circular domains of the opposite sign were found to appear due to polarization backswitching. The obtained results can be used for practical applications of domain and domain wall engineering in ferroelectrics.

**Keywords:** relaxor ferroelectrics, strontium barium niobate, polarization reversal, scanning probe microscopy, domain shape

Corresponding Author: E.A. Neradovskaya; email: neradovskaia.elizaveta@ya.ru

Received: 9 September 2016  
Accepted: 19 September 2016  
Published: 12 October 2016

Publishing services provided  
by Knowledge E

© E.A. Neradovskaya et al. This article is distributed under the terms of the [Creative Commons Attribution License](#), which permits unrestricted use and redistribution provided that the original author and source are credited.

Selection and Peer-review under the responsibility of the ASRTU Conference Committee.

## 1. Introduction

Relaxor ferroelectrics (relaxors) possess unique properties interesting from both fundamental science and practical application points of view. Strontium barium niobate  $\text{Sr}_x\text{Ba}_{x-1}\text{Nb}_2\text{O}_6$  (SBN) single crystals possessing high electrooptic, nonlinear-optic, piezoelectric, and pyroelectric properties [1] are known as a model relaxors for both experimental and theoretical studies. The improvement of the above mentioned properties can be achieved by the creation of the controlled domain structures. The understanding of the domain shape and domain evolution is thus important for the improvement of functionality of tailored domain patterns.

Local polarization reversal in ferroelectrics by application of dc voltage using conductive tip of scanning probe microscope (SPM) is one of the most promising methods for the creation of microdomain arrays in ferroelectrics. This technique consists of application the local electric field and visualization of the created domains with nanometer spatial resolution. A large amount of papers are devoted to the investigation of the local polarization reversal in various ferroelectrics, such as lithium niobate [2-4], but domain kinetics in relaxors is still insufficiently studied.

It is well known that the relaxor characteristics are strongly dependent on the pre-history (in non-ergodic state), and the sequence of the application of electric field and temperature change are important, as well as the initial domain state. However, the

## OPEN ACCESS

known studies of the local reversal polarization in SBN crystals [5-7] have not taken into account the influence of the initial domain structure.

In this work, we present the study of the influence of the initial domain state on the shape and sizes of the isolated domain during local polarization reversal in SBN crystals doped by Ce and Ni.

## 2. Methods

The studied relaxor single crystals  $\text{Sr}_{0.61}\text{Ba}_{0.39}\text{Nb}_2\text{O}_6$  doped with 0.004%  $\text{CeO}_2$  (SBN61:Ce) and 0.01%  $\text{Ni}_2\text{O}_3$  (SBN61:Ni) were grown by modified Stepanov technique [8]. The 0.5 and 1.0-mm-thick plates were cut perpendicular to the polar axis and polished. Freezing temperature  $T_f$  (temperature of transition from ferroelectric to relaxor phase) was between 66 and 79°C and Burns temperature  $T_B$  (temperature of transition from relaxor to paraelectric phase) was about 81-85°C in these crystals. The polarization reversal was performed at room temperature in ferroelectric phase (i.e., at  $T < T_f$ ).

Three types of the initial domain structures have been used for the investigation: (1) "as-grown", (2) "nanodomain", and (3) "single domain" states. As-grown structure appeared after sample polishing without any application of an electric field. Nanodomain structure was created by thermal depolarization using zero-field cooling from 200°C ( $T > T_B$ ). Single domain state was created by slow in-field heating under constant external field ranged from 400 V/mm (for SBN61:Ce and SBN61:Ni) to 500 V/mm (for SBN61:Ni only). Samples were slowly heated, annealed at 200°C during 2 hours, slowly cooled, and left at room temperature for 10 h under dc field. The heating and cooling rates were about 5 K/min.

For all initial domain structures the polarization reversal has been done by application of *dc* voltage pulses [10] with amplitudes ranged from 1 to 150 V and duration – from 0.1 to 1024 s via conductive SPM tip. Resulting static domain structure was visualized by piezoresponse force microscopy (PFM) using scanning probe microscope Asylum MFP-3D (Oxford Instruments, UK) with silicon NSC-18 tips (MikroMash, Estonia). The tips had platinum conductive coating and typical radius of curvature of about 25 nm.

It is known that the polar component of the field produced by the tip is essentially nonuniform (Fig. 1). The field distribution in ZX plane has been calculated by the following equation [11]:

$$E_{ZX} = \frac{C_t U_{sw}}{2\pi\epsilon_0\gamma \left( \sqrt{\epsilon_c\epsilon_a} + 1 \right)} \frac{z/\gamma - z_0}{\left[ (x-x_0)^2 + (y-y_0)^2 + (z/\gamma - z_0)^2 \right]^{3/2}}, \quad (1)$$

where  $C_t$  is the capacitance of the probe (2),  $\epsilon_a$  and  $\epsilon_c$  are the dielectric constants along the polar and nonpolar axes, respectively, and  $U_{sw}$  is the switching voltage,  $\gamma = \sqrt{\epsilon_c/\epsilon_a}$ .

$$C_t = 4\pi\epsilon_0 r_{tip} \frac{1 + \sqrt{\epsilon_c\epsilon_a}}{1 - \sqrt{\epsilon_c\epsilon_a}} \log \frac{2}{1 + \sqrt{\epsilon_c\epsilon_a}}, \quad (2)$$

where  $r_{tip}$  is the radius of tip curvature.

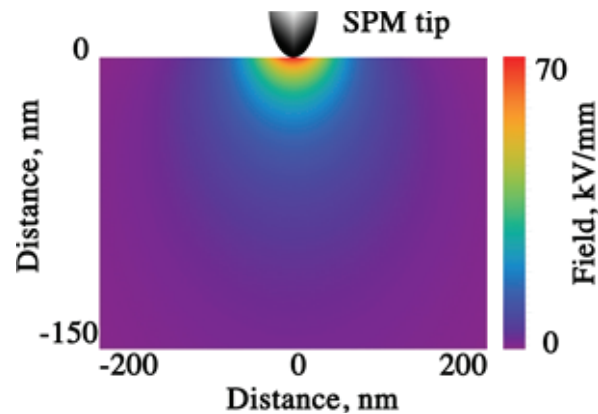


**Figure 1:** The calculated ZX distribution of the field, produced by SPM tip in contact with the polar surface of SBN61 ( $\epsilon_c = 900$ ,  $\epsilon_a = 450$ ,  $r_{tip} = 25$  nm,  $U_{sw} = 100$  V).

Two ways of pulse application for polarization reversal were performed: (1) “with withdrawal”, when the voltage pulse ends simultaneously with tip withdrawal from the sample surface, and (2) “without withdrawal”, when the pulse ends in about 0.1 s before the tip withdrawal.

It should be mentioned that the sizes of the formed domains depend on the relative humidity of the environment. It could be explained by the presence of water layer at the surface and appearance of the water meniscus in the vicinity of the tip [12, 13]. Our experiments were performed at the relative humidity  $35 \pm 5$  %.

One more parameter, which influences the domain size, is a distance between isolated domains in the created array [14]. We considered the case, when the field produced by the first domain did not affect the polarization reversal of the neighboring one. This distance was measured experimentally by adjusting the distance between subsequent positions of the tip, for which all domains in array produced with the same switching parameters have approximately the same size. The  $10\text{-}\mu\text{m}$ -distance was chosen for low voltage pulses (10-50 V) and the  $15\text{-}\mu\text{m}$ -distance was chosen for high voltage amplitudes (60-150 V). Afterwards, the stability of the produced domain structures was studied by serial PFM scanning of the array.

### 3. Results

In this work, all three initial domain states were investigated. It was shown that the as-grown domain structure represented a fractal-type 3D maze (Fig. 2a) with fractal dimension  $D = 1.7$  for SBN61:Ce and  $D = 1.8$  for SBN61:Ni. Thus obtained  $D > 1.5$  indicates that formation of as-grown domain structure is a correlated process. The Fourier analysis of the structure revealed that it is quasiperiodic with the averaged period 200-300 nm.

Thermal depolarization leads to the formation of nanodomain structure, which pattern is changed slowly and after several days becomes very similar to the as-grown one. To create the artificial domains we applied dc electric field immediately after thermal depolarization.

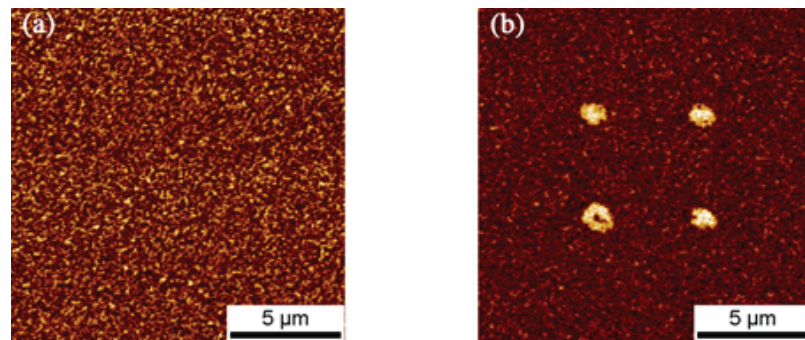


**Figure 2:** (a) As-grown domain structure; (b) domains formed by voltage pulse with tip withdrawal in as-grown structure. SBN61:Ni.  $U_{sw} = 50$  V,  $t = 1$  s.

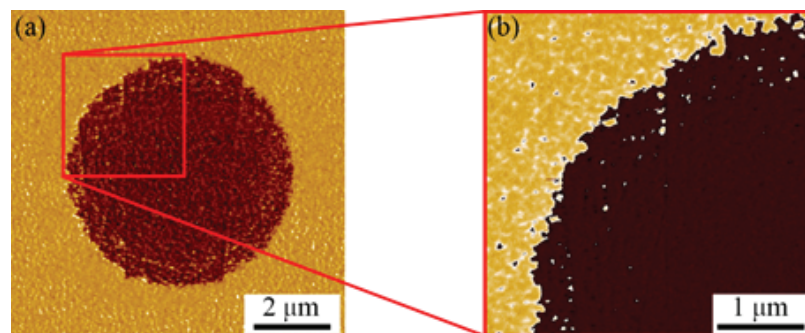


**Figure 3:** Typical circular shape of the domain formed by voltage pulse with tip withdrawal in SBN61 in nanodomain state.  $U_{sw} = 100$  V,  $t = 1$  s.

The “single domain” state obtained after referred procedure was typically unstable. The most stable state has been achieved after exposure to the electric field of 500 V/mm during 12-16 hrs. Switching of this state was investigated by PFM.

### 3.1. As-Grown Domain State

Application of rectangular pulses with  $U_{sw} = 50$  V and  $t = 1$  s with tip withdrawal led to formation of irregular shape domains (Fig. 2b). It should be noted that the first domain (lower left) is larger than its neighbors due to interaction between domains produced at the distance  $5 \mu\text{m}$  from each other. It is known that the depolarization field produced by existing domain decreases the applied field value in its vicinity.

### 3.2. Nanodomain State

The formation of circular domains was attempted for nanodomain state (Fig. 3a). We hypothesized that the domain wall shape (Fig. 3b) was determined by the presence of nanodomains, which merged with the moving wall driven by applied field. We stress that random position of the steps at the domain wall generated by merging (Fig. 3b) is equivalent to stochastic nucleation [15, 16].

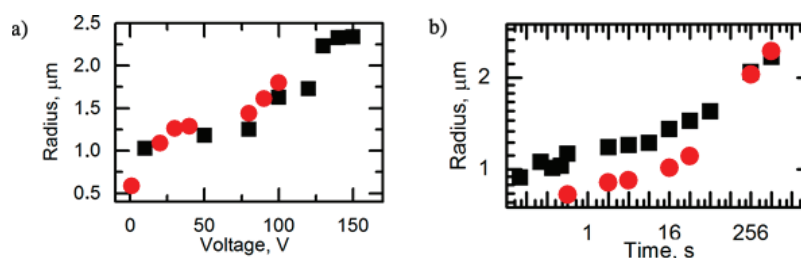


**Figure 4:** The dependences of the averaged domain radius on (a) voltage and (b) pulse duration for nanodomain state: SBN61:Ce (red circles); SBN61:Ni (black squares). (a)  $t_{sw} = 1$  s, (b)  $U_{sw} = 100$  V.

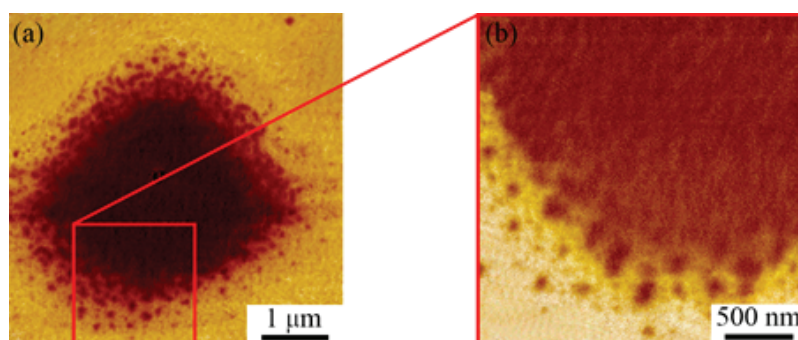


**Figure 5:** Typical domain shape obtained in SBN61:Ce in single domain state by dc voltage pulse with the tip withdrawal.

It is shown that the nanodomain state is very sensitive to the application of a weak field during domain visualization by piezoresponse force microscopy. Switching of nanodomains at the surface was obtained even for driving amplitude as small as 300 mV. The main feature of nanodomain state is related to the ability to produce domains by application of the electric field of both polarities.

The time (Fig. 4a) and voltage (Fig. 4b) dependences of the domain radius have been obtained for nanodomain state in SBN61:Ni and SBN61:Ce. Similar dependences have been obtained for both samples.

### 3.3. Single Domain State

The irregular domain shape was obtained also for single domain state (Fig. 5a). Nanodomains have been observed in a wide layer in front of the moving domain wall ("broad domain boundary", BDB [16]). The BDB in single domain state is essentially wider (about one micron) (Fig. 5b) as compared to the case of nanodomain state (about 200 nm) (Fig. 3b).

Fast relaxation of the artificially created domain structure was observed in both samples in single domain state. Domain structure formed by  $U_{sw} = 100$  V and  $t_{sw} = 1$  s disappeared with relaxation time of about 12 min (Fig. 6).

Typical shape of the domain formed by application of dc voltage  $U_{sw} = 50$  V and  $t_{sw} = 1$  s without tip withdrawal in SBN61:Ce is shown in Fig. 7a. A backswitched domain was observed in the center of the formed domain. The backswitching occurred due to injection of charge carriers from the tip and ineffective screening of the initial field. The

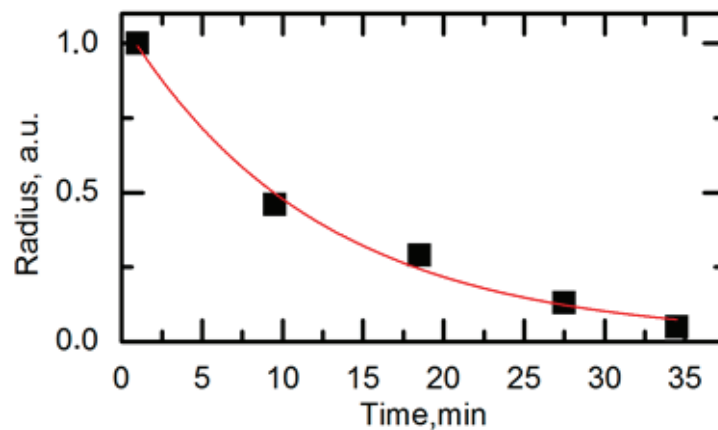


**Figure 6:** Relaxation of the radius of domain formed in SBN61:Ni in single domain state by dc voltage pulse with tip withdrawal.  $U_{sw} = 100$  V,  $t_{sw} = 1$  s. Experimental points fitted by exponential decay.

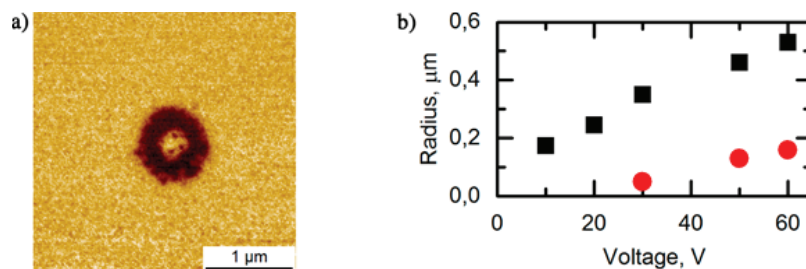


**Figure 7:** Backswitching of the domain formed by application dc voltage without tip withdrawal in SBN61:Ce in single domain state: (a) domain shape for  $U_{sw} = 50$  V and  $t_{sw} = 1$  s; (b) voltage dependence of the averaged domain radius for  $U_{sw} = 100$  V and  $t_{sw} = 32$  s (black squares) and averaged radius of backswitched domain (red circles).

size of backswitched domain increased with increasing of the applied voltage (Fig. 7b). Detailed explanation of the backswitching effect observed by SPM in ferroelectrics can be found elsewhere [17]. In order to understand the detailed mechanism of polarization backswitching in relaxors, further measurements are needed.

## 4. Conclusions

The influence of the initial domain state on the parameters of isolated domains created by local polarization reversal by the conductive tip of scanning probe microscope was studied in SBN single crystals doped with Ce and Ni. It was demonstrated that the domain shape strongly depended on the initial domain structure and domain radius increased with increasing amplitude and duration of the voltage pulse. Circular domains of the opposite sign were found to appear due to polarization backswitching. The obtained relations between the domain shape and the initial domain structure can be used for domain engineering and domain wall engineering in relaxor crystals [18].



## Acknowledgement

The equipment of the UCSU "Modern Nanotechnology", UrFU has been used. The research was supported by Government of the Russian Federation (Act 211, Agreement 02.A03.21.0006) and the Russian Foundation of Basic Research (grant 16-02-00821-a).

## References

- [1] R. R. Neurgaonkar and L. E. Cross, Piezoelectric tungsten bronze crystals for SAW device applications, *Materials Research Bulletin*, **21**, no. 8, 893–899, (1986).
- [2] B. J. Rodriguez, R. J. Nemanich, A. Kingon, A. Gruverman, S. V. Kalinin, K. Terabe, X. Y. Liu, and K. Kitamura, Domain growth kinetics in lithium niobate single crystals studied by piezoresponse force microscopy, *Applied Physics Letters*, **86**, no. 1, Article ID 012906, 1–12906, (2005).
- [3] G. Rosenman, P. Urenski, A. Agronin, Y. Rosenwaks, and M. Molotskii, Submicron ferroelectric domain structures tailored by high-voltage scanning probe microscopy, *Applied Physics Letters*, **82**, no. 1, 103–105, (2003).
- [4] A. V. Ilevlev, A. N. Morozovska, E. A. Eliseev, V. Y. Shur, and S. V. Kalinin, Ionic field effect and memristive phenomena in single-point ferroelectric domain switching, *Nature Communications*, **5**, article no. 4545, (2014).
- [5] T. R. Volk, R. V. Gainutdinov, Y. V. Bodnarchuk, L. V. Simagina, E. D. Mishina, N. A. Ilyin, V. V. Artemov, and L. I. Ivleva, Microdomain arrays fabricated in strontium-barium niobate crystals by microscopic methods, *Ferroelectrics*, **442**, no. 1, 63–73, (2013).
- [6] Y. Bodnarchuk, R. Gainutdinov, S. Lavrov, T. Volk, F. Chen, and H. Liu, Fabrication of Microdomains and Microdomain Patterns by AFM Method in He-Implanted Optical Waveguides on Strontium-Barium Niobate Crystals, *Ferroelectrics*, **485**, no. 1, 1–12, (2015).
- [7] R. V. Gainutdinov, T. R. Volk, O. A. Lysova, I. I. Razgonov, A. L. Tolstikhina, and L. I. Ivleva, Recording of domains and regular domain patterns in strontium-barium niobate crystals in the field of atomic force microscope, *Applied Physics B: Lasers and Optics*, **95**, no. 3, 505–512, (2009).
- [8] L. I. Ivleva, Physicochemical and technological peculiarities of multicomponent oxide crystal growth from melt by modified Stepanov technique, *Bulletin of the Russian Academy of Sciences: Physics*, **73**, no. 10, 1338–1340, (2009).
- [9] EA. Kolchina, MM. Neradovskiy, VA. Shikhova, DV. Pelegov, VYa. Shur, LI. Ivleva, and J. Dec, Formation of single domain state and spontaneous backswitching in SBN single crystal
- [10] K. Terabe, S. Higuchi, S. Takekawa, M. Nakamura, Y. Gotoh, and K. Kitamura, Nanoscale domain engineering of a  $\text{Sr}_{0.61}\text{Ba}_{0.39}\text{Nb}_2\text{O}_6$  single crystal using a scanning force microscope, 83–89
- [11] EJ. Mele, Screening of a point charge by an anisotropic medium: Anamorphoses in the method of images, *Am. J. Phys.*, **69**, no. 5, 557–562, (2001).
- [12] A. V. Ilevlev, A. N. Morozovska, V. Y. Shur, and S. V. Kalinin, Humidity effects on tip-induced polarization switching in lithium niobate, *Applied Physics Letters*, **104**, no. 9, Article ID 092908, (2014).
- [13] V. Y. Shur, A. V. Ilevlev, E. V. Nikolaeva, E. I. Shishkin, and M. M. Neradovskiy, Influence of adsorbed surface layer on domain growth in the field produced by conductive tip of scanning probe microscope in lithium niobate, *Journal of Applied Physics*, **110**, no. 5, Article ID 052017, (2011).
- [14] A. V. Ilevlev, S. Jesse, A. N. Morozovska, E. Strelcov, E. A. Eliseev, Y. V. Pershin, A. Kumar, V. Y. Shur, and S. V. Kalinin, Intermittency, quasiperiodicity and chaos in probe-induced ferroelectric domain switching, *Nature Physics*, **10**, no. 1, 59–66, (2013).
- [15] V. Y. Shur, Domain engineering in lithium niobate and lithium tantalate: Domain wall motion, *Ferroelectrics*, **340**, no. 1, 3–16, (2006).
- [16] V. Y. Shur, Kinetics of ferroelectric domains: Application of general approach to  $\text{LiNbO}_3$  and  $\text{LiTaO}_3$ , *Journal of Materials Science*, **41**, no. 1, 199–210, (2006).
- [17] A. L. Kholkin, I. K. Bdikin, V. V. Shvartsman, and N. A. Pertsev, Anomalous polarization inversion in ferroelectrics via scanning force microscopy, *Nanotechnology*, **18**, no. 9, Article ID 095502, (2007).
- [18] V. Y. Shur, Kinetics of polarization reversal in normal and relaxor ferroelectrics: Relaxation effects, *Phase Transitions*, **65**, no. 1–4, 49–72, (1998).